Realising Robust Low Speed Sensorless PMSM Control Using Current Derivatives Obtained from Standard Current Sensors

Dr David Hind[1], Chen Li[1], Prof Mark Sumner[1], Prof Chris Gerada[1]
[1]Power Electronics, Machines and Control (PEMC) Group, University of Nottingham, Nottingham, UK

***Abstract*—This paper describes the implementation of a simple, robust and cost-effective sensorless control technique for PMSM machines. The method uses stator current derivative measurements made in response to certain PWM vectors. In this work the derivatives are created from measurements made with standard hall-effect sensors (at the start and end of switching vectors), meaning that specialist transducers, such as Rogowski Coils, are not required. However, under narrow PWM vectors high frequency (HF) oscillations can disrupt the current and current derivative responses. In previous work, the time that PWM vectors were applied to the machine for was extended to a threshold known as the minimum pulse width (t_{min}) in order to allow the HF oscillations to decay and a derivative measurement to be obtained. This introduces additional distortion to the motor current. It is shown here that an artificial neural network can be used to estimate derivatives using measurements from a standard current sensor before the HF oscillations have fully decayed, thus permitting a reduction of the minimum pulse width (and associated distortion).**

Keywords— Sensorless Control; Current derivative; Neural Network; Saliency; PMSM; Permanent Magnet;

I. INTRODUCTION

A long term aim for high performance AC drive systems has been to remove the shaft mounted encoder and estimate the shaft position from motor terminal quantities. Approaches based on mathematical models of the machine can work very well at higher speed but fail at low and zero speed as essential information becomes buried in noise due to low SNR. Various methods have been proposed which inject high frequency sinusoidal or other shaped waveforms to excite saliency responses [1-3], but these introduce additional torque ripple and acoustic noise. Similar issues arise if test pulses are used (e.g. the INFORM method [5]).

The PWM current derivative (PCD) technique is a saliency tracking technique which uses voltage pulses applied under normal PWM operation as test pulses [6, 7], thus no additional high frequency (HF) signals or test pulses are required. The main drawbacks are that a) specialist current derivative sensors are usually required [8, 9] which are expensive and an additional complexity, and b) a minimum vector/pulse width is required to allow HF oscillations due to parasitic capacitances to decay before a derivative measurement can be made [10].

The authors would like to acknowledge the support provided by the EPSRC Impact Acceleration Account (IAA) for this work.

This paper introduces techniques which address both of these drawbacks. The aim is to create a low-cost sensorless drive which can provide high (and controlled) starting torque, and can control loads at low speed. The techniques are demonstrated on an industrial drive system where the inertia of the load system limits the transient response that can be achieved by the speed controller. Additional limitations due to processing delays incurred by the proposed method are highlighted and potential solutions to enable faster speed control for the sensorless system are suggested. An artificial neural network approach for estimating current derivatives from standard current measurements contaminated with high frequency oscillations is also described. This eliminates the need to wait for HF oscillations to fully decay before taking a current derivative measurement, thus allowing a significant reduction in the minimum pulse width to be achieved.

II. THE PWM CURRENT DERIVATIVE (PCD) TECHNIQUE

The PWM current derivative (PCD) technique uses the standard voltage vectors associated with SVPWM as test pulses [6, 7]. Measurements of the current derivative under certain PWM active and null vectors are used to calculate position scalars, P_a, P_b and P_c [6, 7, 11]. The position scalars allow the position vector components, $P_{\alpha\beta}$, to be calculated from (1) and (2). The rotor position, θ, can then be estimated from (3), where 'n' is the number saliency cycles per revolution [6, 7].

$$P_\alpha = P_a - \frac{P_b}{2} - \frac{P_c}{2} \quad (1)$$

$$P_\beta = \frac{\sqrt{3}}{2}\left(P_b - P_c\right) \quad (2)$$

$$\theta = \frac{1}{n}\tan^{-1}\left(\frac{P_\beta}{P_\alpha}\right) \quad (3)$$

Following inverter switching, high frequency oscillations exist in the current and current derivative waveforms which prevent immediate and accurate measurement of the derivative. For part of the work described here, measurement of the derivative has been delayed until these HF oscillations have decayed, meaning that all PWM vectors (under which a derivative measurement is required) have to be applied for an amount of time (the minimum pulse width) sufficient to allow the high frequency oscillations to decay and a derivative

978-1-5090-4281-4/17/$31.00 ©2017 IEEE

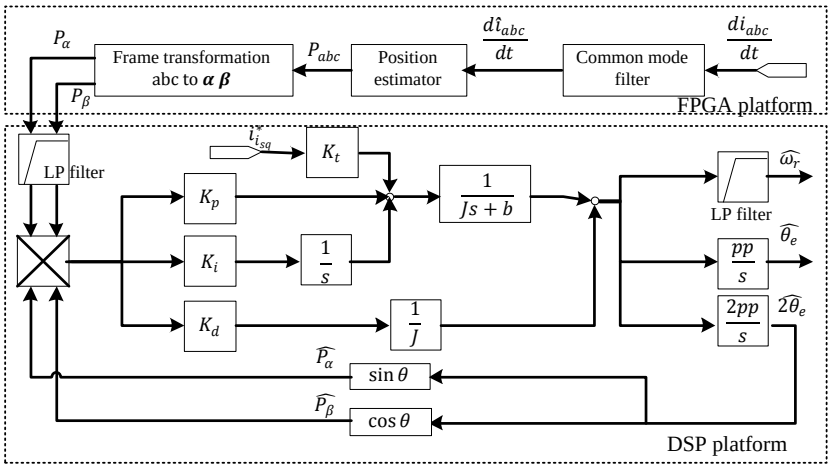

Fig. 1. Block diagram of the sensorless signal processing [4]

measurement to be made [6, 7, 9, 11]. This often involves PWM vector extension (when vectors are less than the minimum pulse width) and subsequent compensation [10], the side effects of which include current distortion, audible noise, torque ripple, vibration and heating. It will be shown later in the paper that by estimating the derivative before the HF oscillations have decayed, that the minimum pulse width and its associated side effects can be reduced.

In an attempt to address the minimum pulse width problem oversampling techniques have previously been applied to extract the derivative from HF contaminated responses in a reduced time. In [9, 11, 12] the derivative response from a dedicated derivative sensor was oversampled and signal-processing was subsequently applied to the response to extract the derivative. The use of standard current sensors was investigated but the length of time required to allow a measureable change in the phase current gradient to occur was found to be excessive. In [13] a recursive least squares curve fit was applied to oversampled current transients. Only offline implementation was discussed and a very high bandwidth current sensor (10MHz) was used. Limited sensor bandwidth and inverter non-linearity would present major problems for both methods.

In this work, a simple method was used for estimating the current derivative. The current derivative is calculated using two current samples obtained over a fixed time window. The first current sample is taken immediately before switching. The second current sample is taken after a fixed time length which allows the high frequency oscillations in the current caused by switching to die down. The method requires that the PWM minimum pulse width be extended, which in turn introduces the undesirable side effects discussed previously (audible noise, torque ripple etc). Through experimental investigation it was found that a 17μs minimum pulse width was sufficient to enable accurate estimation of the derivatives without adding excessive noise to the system.

III. Control Implementation for the Sensorless System

The angle and speed information are obtained as illustrated in Fig. 1. Derivatives are first estimated inside an FPGA, this is because the Artificial Neural Network (ANN) approach (discussed later) required high frequency sampling (62.5MSPS) of the current waveform, an FPGA represented the simplest way of achieving this. Raw current derivatives are then passed to a common mode filter also implemented in the FPGA. A look-up table then translates the derivatives into position scalars, Pabc. From these, position vectors, Pαβ, are calculated according to (1) and (2). These are then passed to a separate DSP where they are first low pass filtered and then supplied to a mechanical observer used to track the saliency angle θe, and extract speed information, ωr, from the position vector [6]. pp is the number of machine pole pairs.

Despite it being possible to use the observed angle directly for orientation, a significant amount of noise and harmonics are present in the observed speed signal, which renders it unsuitable for closed loop speed control. Therefore the

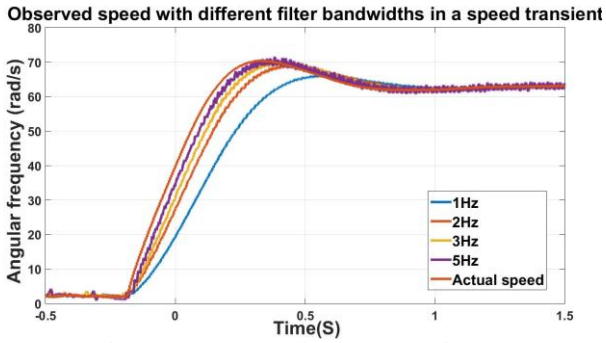

Fig. 2. Low pass filtering removes high frequency noise from speed estimates but also introduces a phase delay as illustrated. A number of cut-off frequencies were tested.

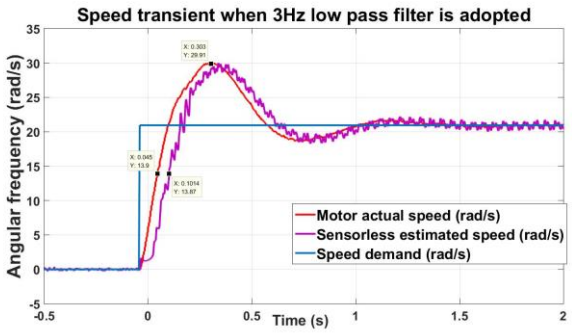

Fig. 3. Speed transient response when 3Hz low pass filter is used

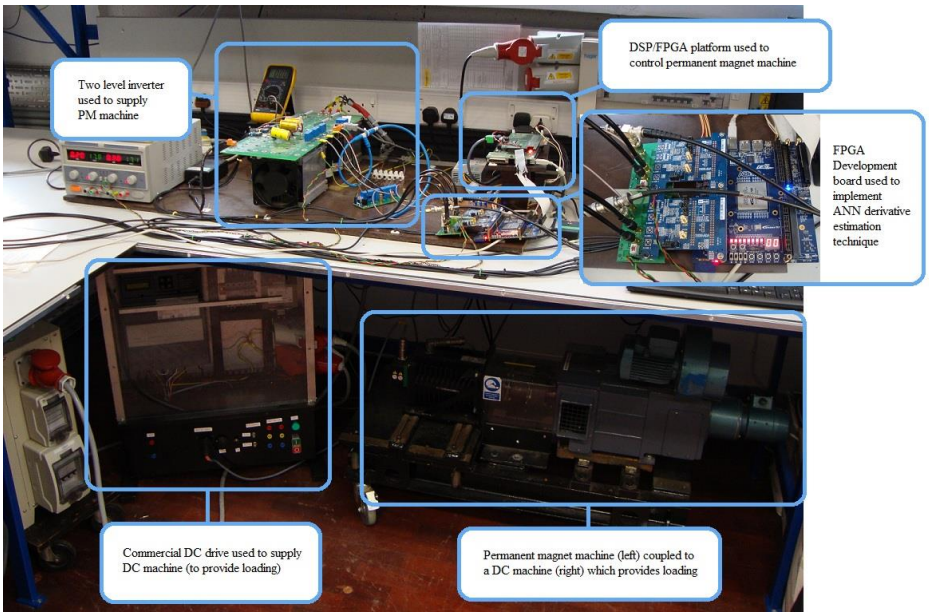

Fig. 4. The experimental system used to evaluate the sensorless control and derivative estimation techniques

captured speed signal is passed to a first order digital low pass filter. As illustrated in Fig. 2, the low pass filter also introduces a large phase delay to the observed speed signal especially when the cut-off frequency is low. This causes the speed loop to be slightly under-damped in sensorless operation. After extensive experimentation, the cut off frequency of the filter was selected to be 3Hz to balance the noise and phase shift whilst offering reasonable performance as illustrated in Fig 3.

IV. Experimental System

The experimental system, illustrated in Fig. 4, consists of a permanent magnet (PM) motor drive coupled to a DC machine and commercial DC drive which provides loading. The parameters of the PM machine are given in Table. 1. The PM drive consists of a two level voltage source inverter and 3.82 kW surface mounted permanent magnet machine controlled by a DSP/FPGA platform. A shaft mounted encoder provides a rotor position measurement. The derivative estimation is implemented on a separate Altera FPGA. The bandwidth of the speed controller in sensored mode is selected to be 2.5Hz, it is limited by the large inertia of the system as well as limited current loop bandwidth caused by extended PWM pulse widths. However in order to provide good performance under sensorless speed control, the bandwidth of the speed controller is further reduced to be 1Hz, given the system's ability to reject noise in the sensorless estimated speed is limited. A block diagram of the control scheme used is given in Fig 5.

V. Experimental Results

A. Sensorless Speed Control

Fig. 6 shows the zero speed performance of the sensorless system in response to full load step changes. The rotor angle and shaft speed are estimated using the sensorless PCD technique with derivatives estimated using two phase current measurements. The system responds according to its design and is stable, returning to its set speed within 0.5s. The speed overshoot is determined by the slow disturbance rejection bandwidth of the control system itself which has been limited by the inertia of the complete system. Similarly Fig. 7 shows the ability of the drive to maintain constant low speed (1 Hz) under load and recover quickly from full load transients. The key points to note here are that a fully functional zero and low speed sensorless drive has been created by utilising relatively crude estimates of current derivatives obtained using standard hall-effect devices. Fig. 8 shows the system response to a step change in speed when the drive is fully loaded. Again a stable and predictable performance is achieved.

TABLE I PM MACHINE PARAMETERS

Rated power	***3.82kW***
Rated speed	***3000rpm***
Rated torque	***12.2Nm***
Rated current	***7.825A***
Pole pairs	***3***
Torque constant	***1.6Nm/A***
Inertia	***20.5e-3 $kg \cdot m^2$***
Line to neutral resistance	***4.7mΩ***
L_s	***4.15mH***

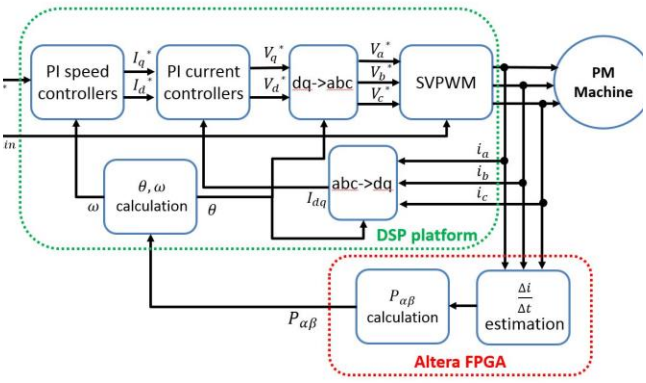

Fig. 5. Block diagram of the control system employed

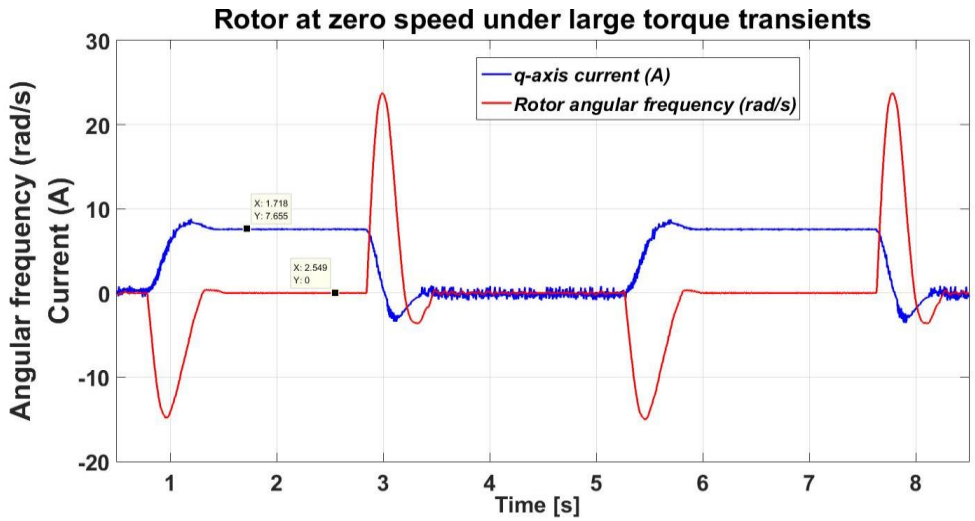

Fig. 6. Full load transients with the drive operating at 0 Hz using two current sample method

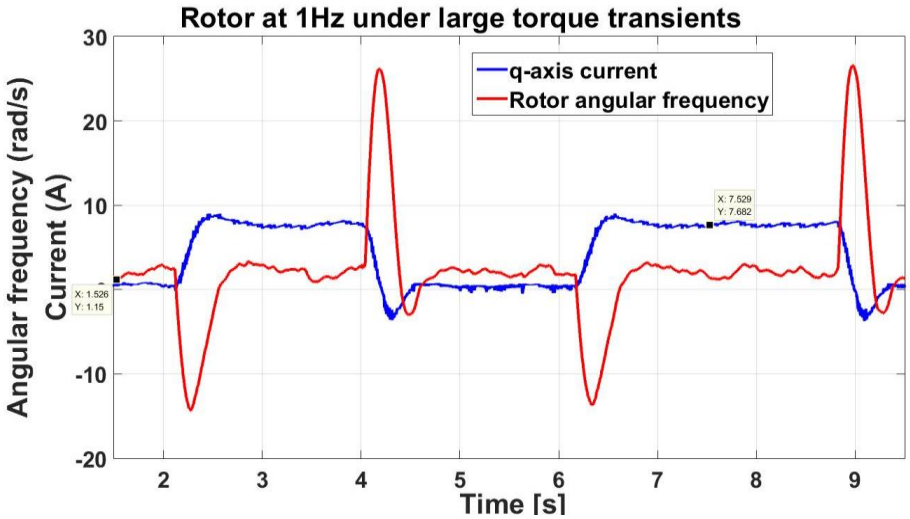

Fig. 7. Full load transients with the drive operating at 1 Hz using two current sample method

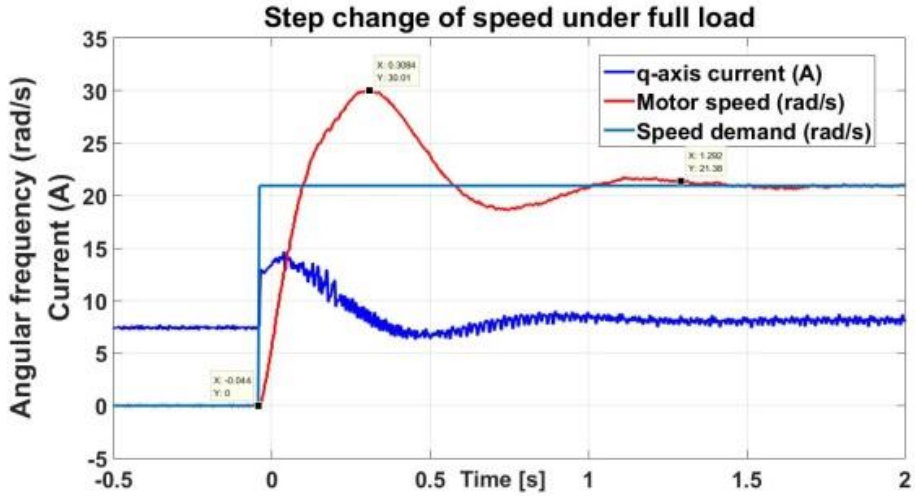

Fig. 8. Speed demand step change (0Hz to 10Hz) when operating at full load

B. *Reducing Audible Noise and Vibration*

Reducing the audible noise and vibration associated with the PCD approach is a key objective for this work. The audible noise associated with the basic drive has been measured using a Brüel & Kjær Type 2236 sound level meter for various minimum vector times (at a 5 kHz switching frequency) and is shown in Fig. 9. It can be seen that a significant reduction in audible noise can be achieved if the minimum pulse time can be reduced to below 5µs.

In order to permit the use of a shorter minimum vector time and still apply the same sensorless position estimation approach, the current derivatives must be measured or estimated in a reduced time. This can be achieved by using a feedforward ANN trained to associate the initial transient current responses with steady state current derivatives. Training of the ANN is achieved offline through the backpropagation algorithm. Training data is required and is captured during a pre-commissioning routine where the machine is operated with a large (20µs) minimum pulse width applied to the first and second active vectors in the first and second halves of the PWM period respectively. Null vectors were found to be sufficient in duration and hence did not require modification. The current response to the applied PWM vectors is sampled at high speed (62.5MSPS) to capture the high frequency transient current response to a reasonable resolution and a large section of the steady state response after the HF oscillations have decayed.

Once a large number of these transients have been collected, a least squares curve fit (according to y=mx+c) is applied to the steady state part of each current response to obtain the derivative which can be used as target data. For each derivative, the first 2µs of the corresponding transient current response is stored as the training data. Details of the training method are further discussed in [14]. Provided the ANN configuration is saved, the pre-commissioning routine is required only once for a given motor drive setup.

An example of the performance of the ANN for derivative estimation is illustrated in Fig 10 where ANN derivative estimates are compared with derivative measurements obtained directly from a derivative sensor. Using the ANN approach the minimum pulse width was reduced from 17µs to 2µs. The reduction in the torque ripple could not be measured directly on the experimental setup available, but an indication is given in Fig 11 which shows measurements of the vibration experienced on the motor's stator casing when minimum pulse widths of 2µs and 18µs are used. The number of vibration modes increases significantly when the larger minimum pulse width is used.

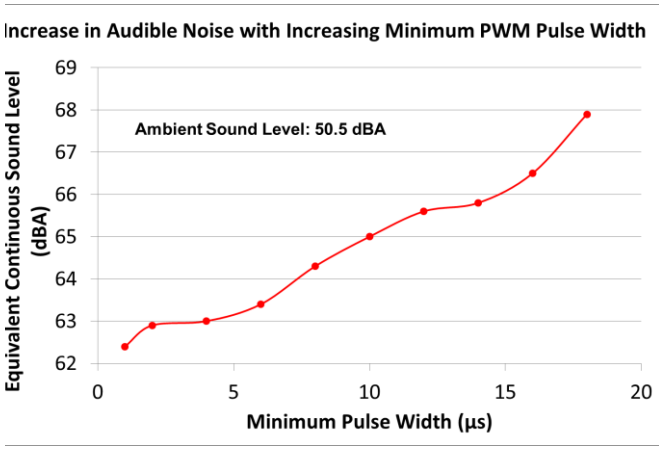

Fig. 9. Equivalent Continuous Sound Level at various minimum PWM vector pulse widths

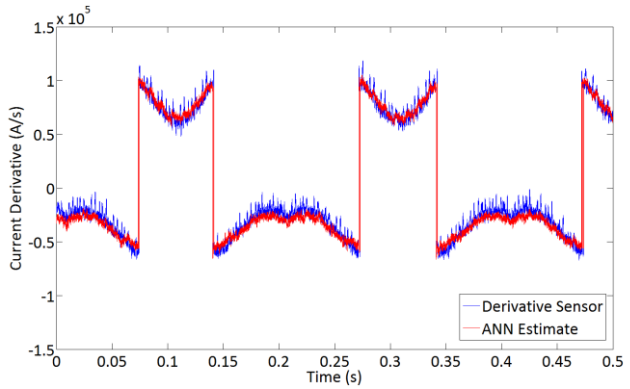

Fig. 10. Comparison of di/dt from dedicated derivative sensor (blue) and ANN estimate (red)

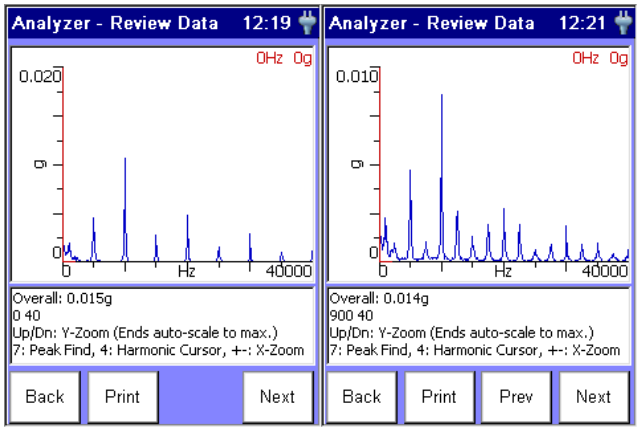

Fig. 11. Vibration experienced on stator casing with a) 2µs minimum vector and b) 18µs minimum vector time

VI. Conclusion

This paper has described the implementation a sensorless control method which uses current derivatives obtained indirectly using standard hall-effect current sensors. The experimental results show that this rather crude approach to estimating current derivatives still provides good torque production and controllability of the shaft speed in response to full load torque step changes. Disturbances in the estimated rotor position angle mean that the speed estimate derived from the sensorless technique cannot be used directly and instead must first be filtered. The addition of a filter limits the dynamic response of the system. If the disturbances in the rotor angle estimate could be reduced, the filtering requirement could be reduced or removed completely.

To allow the sensorless PCD method to operate with measurements made under narrow minimum pulse widths

(2µs) using standard Hall Effect current sensors, a method for estimating derivatives using an artificial neural network supplied with current measurements was presented. It was shown that this method can estimate derivatives successfully under narrow pulse widths. Also, reducing the minimum pulse width measurably reduces the audible noise and vibration experienced in around the drive.

REFERENCES

[1] G. Xie, K. Lu, S. K. Dwivedi, J. R. Rosholm, and F. Blaabjerg, "Minimum-Voltage Vector Injection Method for Sensorless Control of PMSM for Low-Speed Operations," *IEEE Transactions on Power Electronics*, vol. 31, pp. 1785-1794, 2016.

[2] D. Kim, Y. C. Kwon, S. K. Sul, J. H. Kim, and R. S. Yu, "Suppression of Injection Voltage Disturbance for High-Frequency Square-Wave Injection Sensorless Drive With Regulation of Induced High-Frequency Current Ripple," *IEEE Transactions on Industry Applications*, pp. 302-312, 2016.

[3] T. C. Lin and Z. Q. Zhu, "Sensorless Operation Capability of Surface-Mounted Permanent-Magnet Machine Based on High-Frequency Signal Injection Methods," *IEEE Transactions on Industry Applications*, vol. 51, pp. 2161-2171, 2015.

[4] M. W. Degner and R. D. Lorenz, "Using multiple saliencies for the estimation of flux, position, and velocity in AC machines," in *Industry Applications Conference, 1997. Thirty-Second IAS Annual Meeting, IAS '97., Conference Record of the 1997 IEEE*, 1997, pp. 760-767 vol.1.

[5] M. Schroedl, "Sensorless control of AC machines at low speed and standstill based on the "INFORM" method," in *Industry Applications Conference, 1996. Thirty-First IAS Annual Meeting, IAS '96., Conference Record of the 1996 IEEE*, 1996, pp. 270-277 vol.1.

[6] H. Yahan, G. M. Asher, M. Sumner, and Q. Gao, "Sensorless Control of Surface Mounted Permanent Magnetic Machine Using the Standard Space Vector PWN," in *Industry Applications Conference, 2007. 42nd IAS Annual Meeting. Conference Record of the 2007 IEEE*, 2007, pp. 661-667.

[7] Q. Gao, G. M. Asher, M. Sumner, and P. Makys, "Sensorless Control of Induction Machines, including Zero Frequency using only Fundamental PWM Excitation," in *IEEE Industrial Electronics, IECON 2006 - 32nd Annual Conference on*, 2006, pp. 793-798.

[8] P. Nussbaumer and T. M. Wolbank, "Using oversampling techniques to extract ac machine saliency information," in *IECON 2010 - 36th Annual Conference on IEEE Industrial Electronics Society*, 2010, pp. 1035-1040.

[9] P. Nussbaumer and T. M. Wolbank, "Using switching transients to exploit sensorless control information for electric machines," in *Sensorless Control for Electrical Drives (SLED), 2011 Symposium on*, 2011, pp. 35-40.

[10] Y. Hua, M. Sumner, G. Asher, Q. Gao, and K. Saleh, "Improved sensorless control of a permanent magnet machine using fundamental pulse width modulation excitation," *Electric Power Applications, IET*, vol. 5, pp. 359-370, 2011.

[11] J. Juliet and J. Holtz, "Sensorless acquisition of the rotor position angle for induction motors with arbitrary stator windings," in *Industry Applications Conference, 2004. 39th IAS Annual Meeting. Conference Record of the 2004 IEEE*, 2004, pp. 1321-1328 vol.2.

[12] P. Nussbaumer and T. M. Wolbank, "Saliency tracking based sensorless control of AC machines exploiting inverter switching transients," in *Sensorless Control for Electrical Drives (SLED), 2010 First Symposium on*, 2010, pp. 114-119.

[13] D. Yu and M. Sumner, "A novel current derivative measurement using recursive least square algorithms for sensorless control of permanent magnet synchronous machine," in *Power Electronics and Motion Control Conference (IPEMC), 2012 7th International*, 2012, pp. 1193-1200.

[14] D. Hind, M. Sumner, and C. Gerada, "Estimating current derivatives for sensorless motor drive applications," in *Power Electronics and Applications (EPE'15 ECCE-Europe), 2015 17th European Conference on*, 2015, pp. 1-10.